JACS
JOURNAL OF THE AMERICAN CHEMICAL SOCIETY

Communication

pubs.acs.org/JACS

High-Conductance Pathways in Ring-Strained Disilanes by Way of Direct σ-Si−Si to Au Coordination

Nathaniel T. Kim,[†] Haixing Li,[‡] Latha Venkataraman,*[,†,‡] and James L. Leighton*[,†]

[†]Department of Chemistry, Columbia University, New York, New York 10027, United States

[‡]Department of Applied Physics and Applied Mathematics, Columbia University, New York, New York 10027, United States

Supporting Information

ABSTRACT: A highly conducting electronic contact between a strained disilane and Au is demonstrated through scanning tunneling microscope-based single-molecule measurements. Conformationally locked *cis* diastereomers of bis(sulfide)-anchor-equipped 1,2-disilaacenaphthenes readily form high-conducting junctions in which the two sulfide anchors bind in a bipodal fashion to one gold electrode, providing enough stability for a stable electrical contact between the Si−Si σ bond and the other electrode.

The advent of reliable methods to measure single-molecule conductance through metal−molecule−metal junctions[1−4] has inspired efforts to probe molecular and electronic structure−conductivity relationships as well as the nature of the interaction between the anchor or contact groups and the electrodes.[5] While typically the anchor groups (i.e., sulfides and amines) both mechanically and electronically couple to the electrodes, it has also been demonstrated that different structures within a molecule can serve as mechanical and electronic anchors.[6,7] For example, the work of Su et al.[7] showed that sulfides could serve as a mechanical anchor while a silacyclobutane group formed the electrical anchor, enabling a high conductance pathway through the molecular backbone. Here, in an effort to further explore and elucidate strained silacycle−electrode interactions, we have examined the conductance properties of sulfide-anchor-equipped 1,2-disilaacenaphthenes and found that a bipodal molecule to gold substrate binding mode enables the strained high-energy Si−Si σ bond to form a stable electrical contact without a mechanical anchor.

Bis(thioanisole)-substituted 1,2-disilaacenaphthenes **1** (*trans*) and **2** (*cis*) (Figure 1) were synthesized by adapting known procedures for the synthesis of 1,2-disilaacenaphthenes[8−10] (see the Supporting Information (SI) for details). Though we have thus far been unable to obtain crystals of either **1** or **2**, we calculated their structures.[11] In contrast to acenaphthene, which manifests angle strain at the 1 and 8 positions of the naphthalene, the far longer Si−Si bond (2.35 and 2.29 Å for **1** and **2**, respectively) results in angle strain at silicon (C(Np)−Si−Si bond angles = 92° for both **1** and **2**), which raises the energy of the Si−Si σ bond.

The conductance properties of disilanes **1** and **2** were evaluated using the scanning tunneling microscope-based break junction (STM-BJ) technique[12] (experimental details are provided in the SI). While the *trans* diastereomer **1** showed only a single low-conductance (low-*G*) peak at $4.0 \times 10^{-5} G_0$ attributable to the sulfur-to-sulfur pathway (Figure 2a), the *cis* diastereomer **2** showed a prominent high-conductance (high-*G*) peak at $1.4 \times 10^{-3} G_0$ along with a less prominent low-*G* peak at $1.9 \times 10^{-5} G_0$ (Figure 2b).

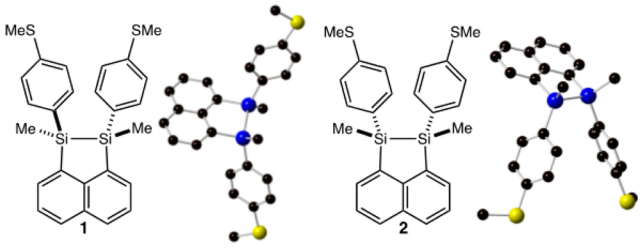

Figure 1. 1,2-Disilaacenaphthenes **1** and **2** and their DFT-optimized structures (H atoms omitted for clarity).

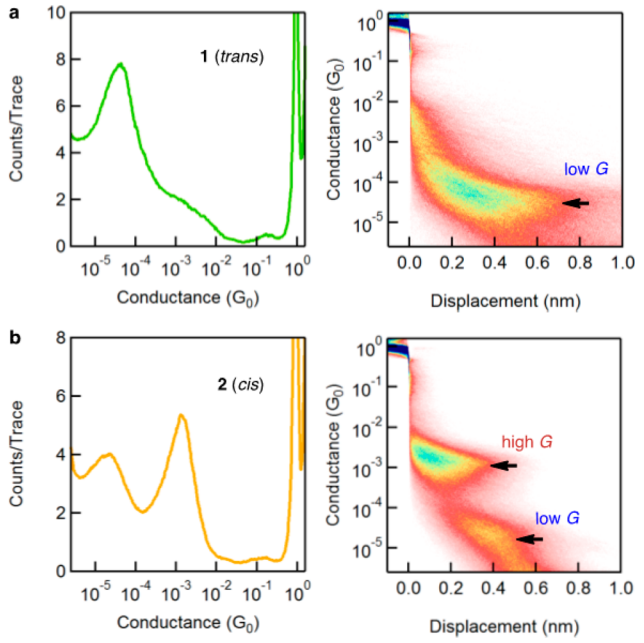

Figure 2. 1D and 2D conductance histograms generated from 13 500 and 20 000 conductance traces measured at an applied voltage of 225 mV with no data selection for (a) *trans* disilane **1** and (b) *cis* disilane **2**.

Received: July 28, 2016
Published: August 26, 2016

DOI: 10.1021/jacs.6b07825
J. Am. Chem. Soc. 2016, 138, 11505−11508

The low-*G* band for **2** could be readily attributed to the sulfur-to-sulfur pathway (Figure 3a), but the origin of the prominent high *G* band was less immediately clear. Past measurements have demonstrated that junction elongation lengths determined from 2D histograms correlate strongly with the molecular backbone length.[13] Thus, the shorter displacement value (~0.4 nm) associated with the high-*G* band is indicative of a conduction path from the silacycle to one of the SMe groups,[7] but a binding arrangement with the nonconducting thioanisole serving as a mechanical anchor on the silacycle-contacting electrode (in analogy to the silacyclobutane) was difficult to envision given the ~4° dihedral angle of the thioanisole groups around the Si–Si bond. Conversely, this rigid coplanar arrangement of the thioanisole groups suggested the possibility that both sulfurs bind to one of the gold electrodes in a bipodal fashion, with the strained high-energy Si–Si σ bond in contact with the other electrode (Figure 3b). Such a bipodal binding mode would be expected to greatly reduce the entropic cost associated with sustaining a stable contact between the weakly donating Si–Si σ bond and the gold electrode. It is possible as well that the naphthyl group and/or the methyl groups provide additional stability through van der Waals interactions with the gold electrode.[14]

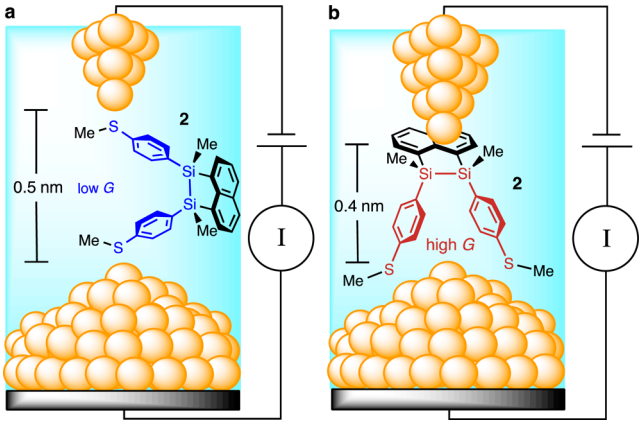

Figure 3. (a) The low-*G* sulfur-to-sulfur junction for **2**. (b) The high-*G* junction with bipodal binding of both thioanisole groups to one gold electrode and the other electrode making direct electrical contact to the Si–Si σ bond.

In an effort to further elucidate the nature of the silacycle–electrode contact, we prepared disilaacenaphthenes **3** (*trans*) and **4** (*cis*) in which one of the thioanisole groups has been replaced with a $-C_6H_4CH_2SCH_3$ group. As shown in Figure 4a, the 1D and 2D histograms for **3** revealed two conductance bands at $1.6 \times 10^{-5} G_0$ and $3.5 \times 10^{-4} G_0$, while the 1D and 2D histograms for **4** showed two similar conductance features at $1.8 \times 10^{-5} G_0$ and $3.4 \times 10^{-4} G_0$ (Figure 4b). In the latter case, it was noted that the first 16 000 traces showed primarily the high-*G* band, while the last 10 000 showed mainly the low-*G* peak. We have previously observed this phenomenon[7] and documented that it may be attributed to a change in concentration, as the solvent (1,2,4-trichlorobenzene) does evaporate to a significant degree over the time scale of the conductance measurements (5–10 h).

As with **1** and **2**, the displacement values associated with the low-*G* peaks of **3** (~0.8 nm) and **4** (~0.6 nm) are consistent with the sulfur-to-sulfur pathways, and as expected because of the addition of a methylene group, they are ~0.1 nm longer than the corresponding values for **1** (~0.7 nm) and **2** (~0.5 nm), respectively. The displacement values associated with the high-*G* peaks are both ~0.4 nm, once again indicative of silacycle-to-sulfide conduits. For **3**, this may be understood as shown in Figure 5a, with the alkyl sulfide serving as a

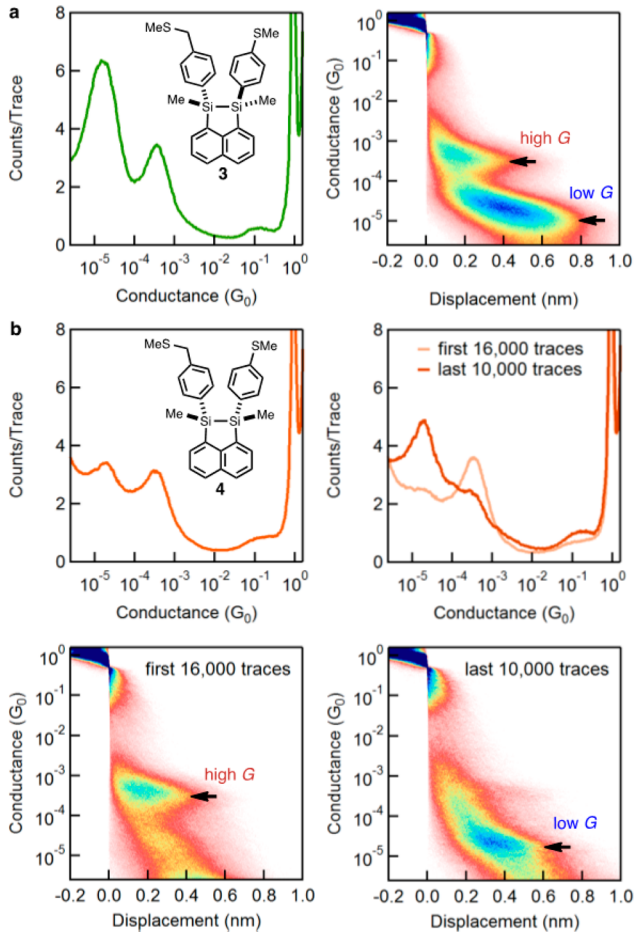

Figure 4. 1D and 2D conductance histograms for (a) *trans* disilane **3** and (b) *cis* disilane **4** (combined traces on the left and traces split into two groups (first 16 000 and last 10 000) on the right).

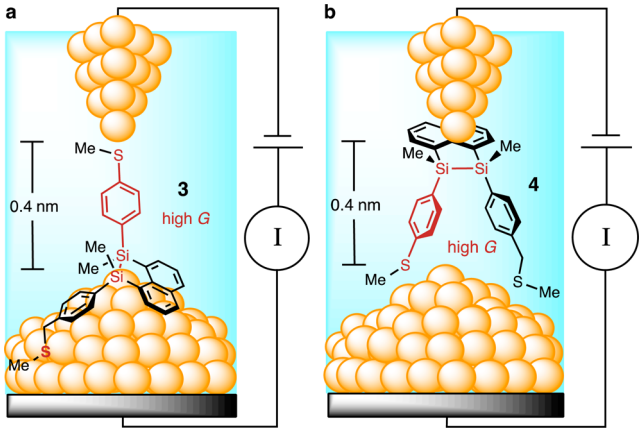

Figure 5. (a) Junction binding model for the high-*G* state of **3**, with mechanical anchoring by the alkyl sulfide stabilizing the weak Si–Si to gold contact. (b) Junction binding model for the high-*G* state of **4**, with bipodal sulfide binding to one electrode stabilizing the weak coupling of the Si–Si bond to the other gold electrode.

DOI: 10.1021/jacs.6b07825
J. Am. Chem. Soc. 2016, 138, 11505–11508

mechanical anchor in analogy to the high-*G* configuration of the silacyclobutane.[7] Conversely, we suggest that the *cis* isomer **4** binds in a bipodal fashion similarly to **2**, with conduction proceeding primarily or exclusively through the thioanisole group (Figure 5b). The significant drop in the high-*G* to low-*G* ratio relative to **2** is easily rationalized within this framework, as the added methylene group is expected to increase the entropic cost of sustaining the weak Si−Si to Au electrical contact, while the observed concentration dependence may be understood as a consequence of the alkyl sulfide binding more strongly to the gold substrate: at high concentrations, the surface is saturated with alkyl sulfides, leaving no available coordination sites for the less strongly binding aryl sulfides.

The conductance switching characteristics of **2**−**4** upon junction elongation support the proposed high-*G* binding configurations. We used a modified ramp in which the high-*G* junction was established and then elongated by 0.2 nm, and we analyzed the impact of elongation on the junction conductance in large data sets of 3000−6000 traces (Figures S1−S4). For **2** and **4**, a switch from the high-*G* state to the low-*G* state was observed in 35% and 37% of the traces, respectively (Table 1),

Table 1. Conductance Switching Data for 2−4 upon 0.2 nm Junction Elongation from the High-*G* States

molecule	high to low	remain high	break
cis **2**	35%	11%	54%
trans **3**	65%	26%	9%
cis **4**	37%	23%	40%

while in the majority of traces the high-*G* junction was either maintained (11% and 23%) or broken (54% and 40%). In contrast, *trans* disilane **3** showed the high-*G* to low-*G* switch in 65% of the traces, in excellent agreement with that seen for the silacyclobutane.[7] In these cases, the energetic cost of the high-*G* to low-*G* switch is expected to be small because the mechanically anchoring sulfide need only slide across the gold surface, consistent with the high frequency of the switch (65%). Conversely, given the proposed bipodal binding configurations, the energetic cost of the high-*G* to low-*G* switch for **2** and **4** is expected to be significantly higher because it requires one of the thioanisole−Au contacts to break and a significant degree of molecular reorientation, consistent with the lower frequency of the high-*G* to low-*G* switch.

The magnitudes of the high-*G* conductance bands for **3** and **4** ($3.5 \times 10^{-4} G_0$ and $3.4 \times 10^{-4} G_0$) are nearly identical though significantly smaller than that of the high-*G* band for **2** ($1.4 \times 10^{-3} G_0$). The proposed high-*G* binding modes for **2**−**4** are consistent with these data, as **3** and **4** conduct primarily or exclusively through a single Si−C_6H_4−SMe pathway (in close analogy to the high-*G* pathway ($4.2 \times 10^{-4} G_0$) for the previously described silacyclobutane[7]) while **2** conducts through two such pathways in parallel (we note here that Breslow, Venkataraman, and Hybertsen have demonstrated that the conductance through parallel components can be more than twice that of the corresponding single-component circuit[15]). Taken together, these data strongly support the conclusion that the primary electrical contact made in the high-*G* binding modes is to the Si−Si σ bond. This makes sense in light of demonstrations of transition-metal-catalyzed additions of the strained Si−Si bond of 1,2-disilaacenaphthenes across reactive π systems[16−18] (e.g., benzyne), which presumably proceed by way of oxidative addition of the Si−Si bond to the metal center and may be preceded by σ complex formation. Indeed, a copper to Si−Si σ complex has been characterized,[19] and oxidative addition of a gold(I) species to a Si−Si bond has been demonstrated.[20,21] Other than the silacyclobutane[7] and the compounds reported here, the only previous report of a direct contact between silicon and a gold substrate is Fichou and co-workers' demonstration that alkynyltrimethylsilanes can form self-assembled monolayers on gold surfaces,[22,23] but the detailed nature of the Si−Au interaction is still under investigation.[24−26] Our work clearly evidences a direct Si to Au contact in single-molecule circuits and provides a well-precedented framework to understand that contact as being a metal to Si−Si bond σ complex.[27]

Though conductance through multipodal (typically tripodal) anchor groups has been demonstrated,[28−31] our work also establishes a new strategy to leverage the reduction in the entropic costs derived from multipodal anchoring to stabilize otherwise too-weak-to-form electrical contacts between weak donors and metal electrodes. This strategy may prove generalizable beyond strained silacycles and may provide a platform to explore reactions such as oxidative addition at the single-molecule level.

■ ASSOCIATED CONTENT

Supporting Information

The Supporting Information is available free of charge on the ACS Publications website at DOI: 10.1021/jacs.6b07825.

Synthetic procedures, STM-BJ procedures, table of conductances, and characterization data (PDF)

■ AUTHOR INFORMATION

Corresponding Authors

*lv2117@columbia.edu

*leighton@chem.columbia.edu

Notes

The authors declare no competing financial interest.

■ ACKNOWLEDGMENTS

We are indebted to our colleagues Dr. Timothy A. Su and Professor Colin Nuckolls for insightful scientific discussions and for the use of Nuckolls group equipment. We thank the National Science Foundation for the primary support of this work under Grant CHE-1404922. H.L. was supported by the Semiconductor Research Corporation and New York Center for Advanced Interconnect Science and Technology Program.

■ REFERENCES

(1) Tao, N. J. *Nat. Nanotechnol.* **2006**, *1*, 173−181.

(2) Moth-Poulsen, K.; Bjørnholm, T. *Nat. Nanotechnol.* **2009**, *4*, 551−556.

(3) Nichols, R. J.; Haiss, W.; Higgins, S. J.; Leary, E.; Martin, S.; Bethell, D. *Phys. Chem. Chem. Phys.* **2010**, *12*, 2801−2815.

(4) Aradhya, S. V.; Venkataraman, L. *Nat. Nanotechnol.* **2013**, *8*, 399−410.

(5) Su, T. A.; Neupane, M.; Steigerwald, M. L.; Venkataraman, L.; Nuckolls, C. *Nat. Rev. Mater.* **2016**, *1*, 16002.

(6) Meisner, J. S.; Kamenetska, M.; Krikorian, M.; Steigerwald, M. L.; Venkataraman, L.; Nuckolls, C. *Nano Lett.* **2011**, *11*, 1575−1579.

(7) Su, T. A.; Widawsky, J. R.; Li, H.; Klausen, R. S.; Leighton, J. L.; Steigerwald, M. L.; Venkataraman, L.; Nuckolls, C. *J. Am. Chem. Soc.* **2013**, *135*, 18331−18334.

(8) Kiely, J. S.; Boudjouk, P. *J. Organomet. Chem.* **1979**, *182*, 173−183.

(9) Ando, W.; Wakahara, T.; Akasaka, T.; Nagase, S. *Organometallics* **1994**, *13*, 4683−4685.
(10) Wakahara, T.; Kodama, R.; Akasaka, T.; Ando, W. *Bull. Chem. Soc. Jpn.* **1997**, *70*, 665−670.
(11) Density functional theory calculations were performed with *Jaguar*, version 8.6 (Schrodinger, LLC: New York, 2014) using the B3LYP functional and the 6-31G** basis sets.
(12) Xu, B.; Tao, N. J. *Science* **2003**, *301*, 1221−1223.
(13) Kamenetska, M.; Koentopp, M.; Whalley, A. C.; Park, Y. S.; Steigerwald, M. L.; Nuckolls, C.; Hybertsen, M. S.; Venkataraman, L. *Phys. Rev. Lett.* **2009**, *102*, 126803.
(14) Aradhya, S. V.; Frei, M.; Hybertsen, M. S.; Venkataraman, L. *Nat. Mater.* **2012**, *11*, 872−876.
(15) Vazquez, H.; Skouta, R.; Schneebeli, S.; Kamenetska, M.; Breslow, R.; Venkataraman, L.; Hybertsen, M. S. *Nat. Nanotechnol.* **2012**, *7*, 663−667.
(16) Yoshida, H.; Ikadai, J.; Shudo, M.; Ohshita, J.; Kunai, A. *J. Am. Chem. Soc.* **2003**, *125*, 6638−6639.
(17) Yoshida, H.; Ikadai, J.; Shudo, M.; Ohshita, J.; Kunai, A. *Organometallics* **2005**, *24*, 156−162.
(18) Yoshida, H.; Nakano, S.; Mukae, M.; Ohshita, J. *Org. Lett.* **2008**, *10*, 4319−4322.
(19) Gualco, P.; Amgoune, A.; Miqueu, K.; Ladeira, S.; Bourissou, D. *J. Am. Chem. Soc.* **2011**, *133*, 4257−4259.
(20) Gualco, P.; Ladeira, S.; Miqueu, K.; Amgoune, A.; Bourissou, D. *Angew. Chem., Int. Ed.* **2011**, *50*, 8320−8324.
(21) Joost, M.; Gualco, P.; Coppel, Y.; Miqueu, K.; Kefalidis, C. E.; Maron, L.; Amgoune, A.; Bourissou, D. *Angew. Chem., Int. Ed.* **2014**, *53*, 747−751.
(22) Marchenko, A.; Katsonis, N.; Fichou, D.; Aubert, C.; Malacria, M. *J. Am. Chem. Soc.* **2002**, *124*, 9998−9999.
(23) Katsonis, N.; Marchenko, A.; Taillemite, S.; Fichou, D.; Chouraqui, G.; Aubert, C.; Malacria, M. *Chem. - Eur. J.* **2003**, *9*, 2574−2581.
(24) Katsonis, N.; Marchenko, A.; Fichou, D.; Barrett, N. *Surf. Sci.* **2008**, *602*, 9−16.
(25) Watcharinyanon, S.; Nilsson, D.; Moons, E.; Shaporenko, A.; Zharnikov, M.; Albinsson, B.; Mårtensson, J.; Johansson, L. S. O. *Phys. Chem. Chem. Phys.* **2008**, *10*, 5264−5275.
(26) Marqués-González, S.; Yufit, D. S.; Howard, J. A. K.; Martín, S.; Osorio, H. M.; García-Suárez, V. M.; Nichols, R. J.; Higgins, S. J.; Cea, P.; Low, P. J. *Dalton Trans.* **2013**, *42*, 338−341.
(27) Crabtree, R. H. *Angew. Chem., Int. Ed. Engl.* **1993**, *32*, 789−805.
(28) Ie, Y.; Hirose, T.; Nakamura, H.; Kiguchi, M.; Takagi, N.; Kawai, M.; Aso, Y. *J. Am. Chem. Soc.* **2011**, *133*, 3014−3022.
(29) Ie, Y.; Tanaka, K.; Tashiro, A.; Lee, S. K.; Testai, H. R.; Yamada, R.; Tada, H.; Aso, Y. *J. Phys. Chem. Lett.* **2015**, *6*, 3754−3759.
(30) Karimi, M. A.; Bahoosh, S. G.; Valásek, M.; Bürkle, M.; Mayor, M.; Pauly, F.; Scheer, E. *Nanoscale* **2016**, *8*, 10582−10590.
(31) Kiguchi, M.; Takahashi, Y.; Fujii, S.; Takase, M.; Narita, T.; Iyoda, M.; Horikawa, M.; Naitoh, Y.; Nakamura, H. *J. Phys. Chem. C* **2014**, *118*, 5275−5283.

DOI: 10.1021/jacs.6b07825
J. Am. Chem. Soc. 2016, 138, 11505−11508